

Neutron irradiation effect on permeability and magnetoimpedance of amorphous and nanocrystalline magnetic materials

Manh-Huong Phan,* Hua-Xin Peng, and Michael R. Wisnom

Department of Aerospace Engineering, Bristol University, Queen's Building, University Walk, Bristol, BS8 1TR, United Kingdom

Seong-Cho Yu

Department of Physics, Chungbuk National University, Cheongju 361-763, Korea

Cheol Gi Kim

ReCAMM, Chungnam National University, Taejon, Chungnam 305-764, Korea

Manuel Vázquez

Instituto de Ciencia de Materiales, CSIC, 28049 Cantoblanco, Madrid, Spain

(Received 20 October 2004; revised manuscript received 14 January 2005; published 28 April 2005)

In this paper we provide physical insights into the effect of neutron irradiation on permeability spectra and magnetoimpedance of amorphous and nanocrystalline alloys. Experimental results indicate that neutron irradiation increases the permeability of the amorphous alloy but decreases the permeability of the nanocrystalline alloy in a high frequency region ($f \geq 1$ MHz), while the opposite is found in a low frequency region ($f < 1$ MHz). A careful examination of sample temperature during neutron irradiation process excludes thermal annealing as a possible origin of the observed irradiation effect. The magnetic relaxations in the low and high frequency regions are ascribed to the irreversible domain wall motion and reversible rotational magnetization, respectively. The enhancement in the permeability of the amorphous alloy upon neutron irradiation leads to a parallel improvement of magnetoimpedance response of the material, which is of practical use for sensing applications.

DOI: 10.1103/PhysRevB.71.134423

PACS number(s): 75.50.Kj, 75.75.+a

Suitable thermomagnetic processing of a metastable amorphous structure leads to parallel evolution of magnetic properties resulting in optimization of their properties. Most conventional procedures to achieve such transformations are performed by annealing at furnace, or under the presence of magnetic fields.¹ In the present work, we investigate a novel processing technique involving neutron irradiation. Despite a number of previous studies,²⁻⁷ the understanding of the neutron irradiation effect on magnetic properties of amorphous and crystalline magnetic alloys remains controversial in part due to the complex nature of the problem. For instance, an increase in the permeability was revealed by relative permeability measurements of an as-quenched amorphous alloy irradiated in a low-field region with a 2.25 MeV proton fluence,^{2,3} was ascribed to the reduction of internal stresses. Brown *et al.*⁴ reported that, for both amorphous and crystalline magnetic alloys, the permeability decreased with increasing neutron fluence as a consequence of the increase of point defects produced by the irradiation and the domain walls pinning at defect clusters created by collision cascade. More recently, however, Kim *et al.*⁷ reported that neutron irradiation decreased the permeability of a nanocrystalline alloy but had a negligible effect on the as-quenched amorphous alloy. It is assumed that this discrepancy might be due to the irradiation with different neutron fluence.^{4,7} Since the magnetization processes⁶ are influenced by external and internal stresses originating at defects,²⁻⁴ the contribution of domain wall motion and rotational magnetization processes to the permeability of neutron irradiated amorphous mag-

netic materials is probably related to the neutron fluence.

To obtain deeper physical insights into the irradiation effect in both amorphous and crystalline materials, we investigated the effect of neutron irradiation on the magnetic properties of amorphous and nanocrystalline alloys by means of complex permeability spectra, magneto-impedance and the dc magnetization process. Amorphous alloy $\text{Fe}_{73.5}\text{Cu}_1\text{Nb}_3\text{Si}_{13.5}\text{B}_9$ ribbons with a thickness of $\sim 20 \mu\text{m}$ and a width of 5 mm were prepared by a rapid quenching technique in vacuum. A subsequent thermal annealing treatment was carried out in vacuum at a temperature of 823 K for 1 h to achieve a stable and homogeneous nanocrystalline state.⁸ Both the amorphous and the nanocrystallized samples were then irradiated for 72 h using a HANARO research reactor at the Korea Atomic Energy Research Institute. The fluxes of thermal (n_{th}) and fast (n_f) neutrons were $3.09 \times 10^{13} n_{th} \text{ cm}^{-2} \text{ s}^{-1}$ and $1.87 \times 10^{11} n_f \text{ cm}^{-2} \text{ s}^{-1}$, respectively. In order to assess the possible thermal annealing effect due to irradiation, some as-quenched amorphous samples were also annealed at 473 K (the maximum sample temperature measured during the neutron irradiation) for 72 h. Magnetoimpedance (MI) and complex permeability were measured using a HP4129A impedance analyzer in the frequency range of $f=0.1-10$ MHz.^{9,10} Magnetization measurements were performed using a vibrating sample magnetometer (VSM).

First, real and imaginary parts of the permeability of an as-quenched amorphous sample (denoted as No. 1) were measured. As shown in Figs. 1(a) and 1(b), at a small exter-

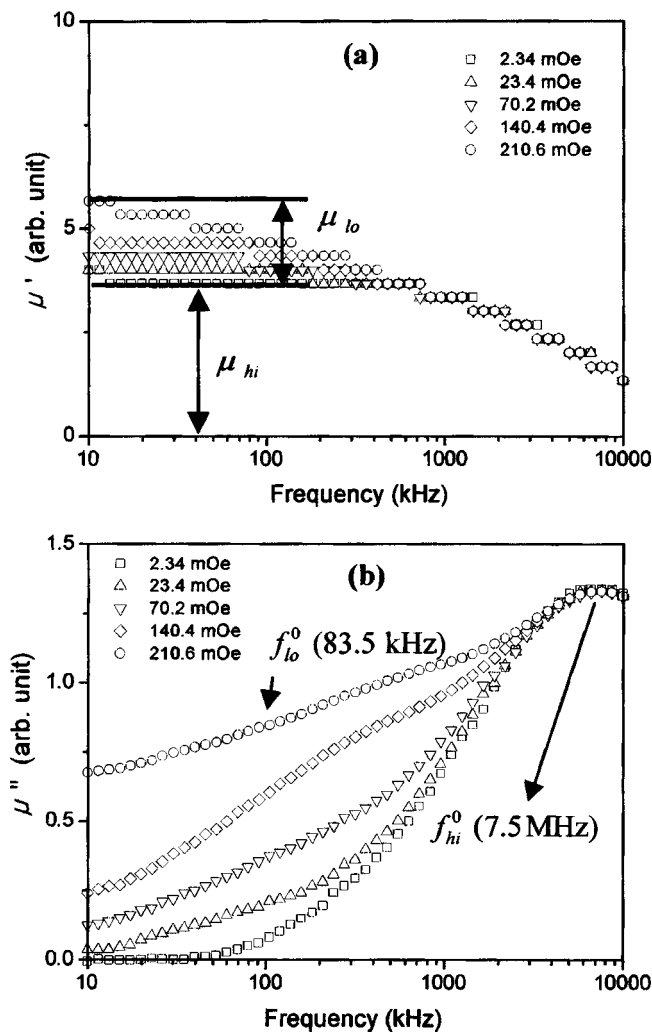


FIG. 1. (a) The real and (b) imaginary parts of the permeability spectra of as-quenched $\text{Fe}_{73.5}\text{Cu}_1\text{Nb}_3\text{Si}_{13.5}\text{B}_9$ sample under different ac fields.

nal field (h_0) of 2.34 mOe, the permeability spectra show a Debye-type relaxation at 7.5 MHz. As the external field exceeds 23.4 mOe, the permeability spectra show an increase in the low-frequency region ($f \leq 1$ MHz). The relaxation region in low frequency was decomposed by subtracting the spectral curve measured at 23.4 mOe from that at 210.6 mOe, where the relaxation frequency was revealed to be

about 83.5 kHz.^{6,10} However, the permeability spectrum in the high-frequency region ($f=7.5$ MHz) does not depend on the external magnetic field. This indicates that a different relaxation process from that observed in high-frequency region has developed in the low-frequency region. Therefore, the complex permeability $\mu^*(f)$ can be expressed by the addition of two decomposed relaxations as follows:

$$\begin{aligned} \mu^*(f) &= \mu'(f) - j\mu''(f) = \mu'_{lo}(f) + \mu'_{hi}(f) - j\{\mu''_{lo}(f) + \mu''_{hi}(f)\} \\ &= 1 + \frac{\mu_{lo}(h_0)}{1 + (f/f_{lo}^0)^2} + \frac{\mu_{hi}(h_0)}{1 + (f/f_{hi}^0)^2} - j \left(\frac{\mu_{lo}(h_0)(f/f_{lo}^0)}{1 + (f/f_{lo}^0)^2} \right. \\ &\quad \left. + \frac{\mu_{hi}(h_0)(f/f_{hi}^0)}{1 + (f/f_{hi}^0)^2} \right), \end{aligned} \quad (1)$$

where μ_{lo} and f_{lo}^0 are the permeability and the relaxation frequency in the low-frequency region, μ_{hi} and f_{hi}^0 are the permeability and the relaxation frequency in the high-frequency region, and h_0 is the amplitude of the ac field. In general, the reversible magnetization process is much faster than the domain wall motion process.^{6,11} The magnetization by domain wall motion shows a threshold field to be activated due to the domain wall pinning at defects. Therefore, the relaxations in low and high frequency regions can be ascribed to the irreversible domain wall motion and the reversible magnetization rotation, respectively.

Following the same experimental procedure, we measured the real and imaginary parts of the permeability of samples: (No. 2) the amorphous ribbon annealed at 473 K, (No. 3) the neutron irradiated amorphous ribbon, (No. 4) the nanocrystalline ribbon, i.e., after annealing the precursor amorphous ribbon at 823 K, and (No. 5) the neutron irradiated nanocrystalline ribbon. For comparison, we summarized, in Table I, the experimental results including the relaxation frequency, f_{lo}^0 and f_{hi}^0 , the initial permeability, μ_{lo} and μ_{hi} , together with the coercivity, H_C , obtained from hysteresis loop measurements and the maximum value of MI measured at 5 MHz.

Comparing sample No. 2 with the amorphous sample No. 1, it can be observed that, after annealing at 473 K, both f_{lo}^0 and f_{hi}^0 decrease slightly whereas μ_{lo} and μ_{hi} increase slightly. That slight increase in the permeability can be attributed to the partial relief of internal stress by annealing at 473 K, but this thermal annealing effect (473 K) is negligible when compared with the effect of neutron irradiation effect

TABLE I. The relaxation frequency, f_{lo}^0 and f_{hi}^0 , the initial permeability, μ_{lo} and μ_{hi} , the coercivity, H_C , and the maximum value of MI ratio, $[\Delta Z/Z]_{max}(\%)$, measured at 5 MHz.

Sample ^a	f_{lo}^0 (kHz)	f_{hi}^0 (MHz)	μ_{lo}	μ_{hi}	H_C (Oe)	$(\Delta Z/Z)_{max}(\%)$
No. 1	83.5	7.5	2.2	4.5	0.14	13.1
No. 2	73.1	6.84	2.4	5.8	0.138	17
No. 3	115	3.6	0.7	8	0.112	24
No. 4	13.9	1.7	0.2	20	0.015	57.1
No. 5	12.1	2	0.45	15	0.095	33.5

^a(No. 1) as-quenched alloy, (No. 2) alloy annealed at 473 K, (No. 3) neutron-irradiated amorphous alloy, (No. 4) alloy annealed at 823 K only, and (No. 5) the 823 K-annealed and neutron irradiated alloy.

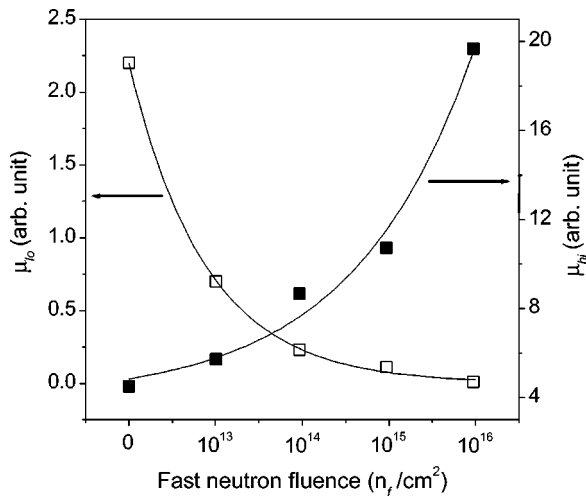


FIG. 2. Changes in initial permeability attributed to the domain wall motion (μ_{lo}) and rotational magnetization (μ_{hi}) as a function of fast neutron fluence. Symbols: open and solid square for experimental data, and solid lines for fitting curve using $\mu = \mu_0 \exp(-g\sigma\epsilon\phi t)$ in Ref. 3.

(see Sample No. 3 in Table I), so excluding the thermal annealing as the origin of the observed neutron irradiation effect.

Comparing the neutron-irradiated sample No. 3 with the as-cast amorphous sample No. 1, a 70% decrease in permeability at low frequencies (μ_{lo}) is concomitant with an 80% increase in permeability at high frequencies (μ_{hi}). This indicates that the pinning force for irreversible wall motion at defects induced by neutron irradiation is increased,⁴ while the contribution to the permeability from the magnetization rotation process is enhanced after neutron irradiation.^{6,10} It is worth noting that the relaxation frequency at low frequencies (f_{lo}^0) increased from 83.5 kHz to 115 kHz after irradiation. As reported earlier,⁴ the decrease in the permeability of the amorphous alloys upon neutron irradiation was attributed to the excessive point defects induced by irradiation and to the pinning of domain walls by defect clusters created by collision cascade. Therefore, the increase of f_{lo}^0 in the present study is likely reflecting an increase in internal stress to hinder the irreversible domain wall motion. But the question is why the parameter f_{hi}^0 of the reversible magnetization decreased from 7.5 MHz to 3.6 MHz after irradiation.

To scrutinize this intriguing feature, we assessed the changes in the relaxation frequency and the initial permeability with neutron fluence. It has been found that f_{lo}^0 increases with neutron fluence, but f_{hi}^0 decreases. The domain wall relaxation frequency is proportional to the pinning force for domain wall motion due to internal stress. In particular, as shown in Fig. 2, the permeability μ_{lo} from low-frequency relaxation decreases exponentially with neutron fluence,⁴ whereas the permeability μ_{hi} from high-frequency relaxation increases. The increase in the high-frequency permeability μ_{hi} can be ascribed to the increase in the volume fraction of domains, which contributes to the rotational magnetization.¹¹ Clearly, the neutron irradiation increases the permeability from reversible magnetization rotation but it decreases the

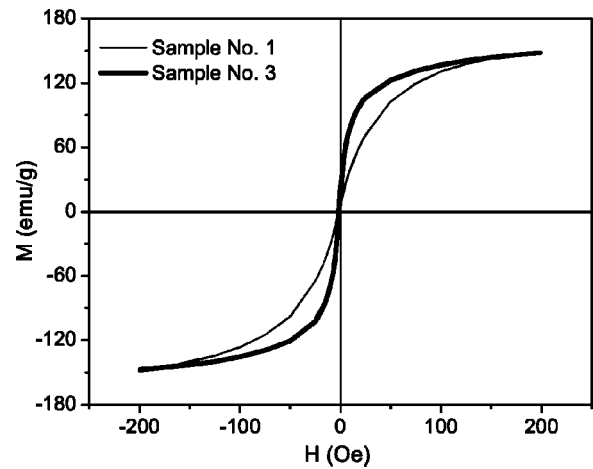


FIG. 3. Hysteresis loops of (No. 1) as-quenched and (No. 3) neutron irradiated samples.

permeability from irreversible domain wall motion in the as-quenched amorphous alloy. As discussed below, these results bring basic physical understanding of the realistic contribution of domain wall motion and rotational magnetization processes to the permeability^{4,7} and thus to the magnetoimpedance.

For the nanocrystalline sample (No. 4), the very large high-frequency permeability can be ascribed to the high rotational contribution and to a negligible local magnetocrystalline anisotropy. The magnitude of μ_{lo} decreased to certain extent, but μ_{hi} increased drastically in comparison to sample No. 1. The drastic increase in the permeability (μ_{hi}) of the nanocrystalline sample is attributed to the structural relaxation caused by the thermal annealing effect.^{5,7} The structural relaxation reduces the residual stress, decreasing the hindrances to domain wall motion.⁴ This explains why f_{lo}^0 decreases from 83.5 kHz for the as-quenched sample (No. 1) to 13.9 kHz for the nanocrystalline sample (No. 4), while for the neutron-irradiated sample (No. 3), f_{lo}^0 increases to 115 kHz. This also suggests that neutron irradiation results in a transient, highly localized energy deposition in opposition to a thermal equilibrium characteristic of thermal annealing process.³

In contrast to its effect in the amorphous alloys, neutron irradiation in the nanocrystalline alloy decreases the permeability from reversible rotational magnetization (μ_{hi}) but increases the permeability from irreversible domain wall motion (μ_{lo}) (see samples No. 4 and No. 5 in Table I). The reduction in the magnetic softness of the nanocrystalline sample due to neutron irradiation is also confirmed by the increase in coercivity of sample No. 5 ($H_c = 0.095$ Oe) compared to sample No. 4 ($H_c = 0.015$ Oe). It is therefore reasonable to claim that neutron irradiation increases the rotational permeability in an amorphous alloy, but decreases the rotational permeability in a nanocrystalline alloy.

Furthermore, the magnetic hysteresis loops (e.g., the M - H curves) in Fig. 3 show that the neutron-irradiated amorphous alloy (sample No. 3) is softer than the amorphous alloy (sample No. 1). It should be noted that the magnetic softness was improved in the as-quenched amorphous

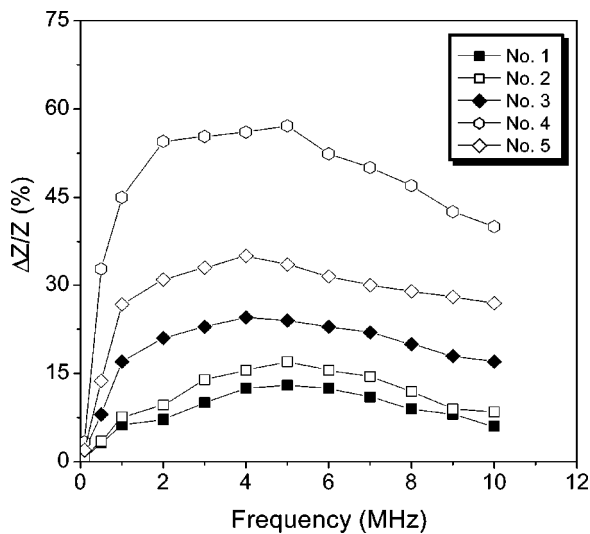


FIG. 4. The measured magnetoimpedance ratio ($\Delta Z/Z$) as a function of frequency. (No. 1) the as-quenched alloy, (No. 2) the alloy annealed at 473 K, (No. 3) the neutron irradiated amorphous alloy, (No. 4) the alloy annealed at 823 K, and (No. 5) the 823 K-annealed and neutron irradiated alloy.

sample after neutron irradiation, but saturation magnetization was insensitive to the irradiation effect (see Fig. 3). No noticeable change of hysteresis loop was found in the sample annealed at 473 K for 72 h (sample No. 2), indicating that this annealing condition did not significantly affect the magnetic softness, and that the change in the M - H curve of sample No. 3 (Fig. 3) was caused solely by neutron irradiation. These results indicate that such an improvement in the magnetic softness of the as-quenched amorphous alloy subjected to neutron irradiation is likely due to the enhancement of rotational magnetization. In connection with the permeability data, we can attribute the increased permeability in the as-quenched amorphous alloy upon neutron irradiation (sample No. 3) to the enhancement of rotational magnetization.

Finally, to complete the analysis, we measured the magnetoimpedance ratio ($\Delta Z/Z = [Z(H) - Z(H_{max})]/Z(H_{max})$) as a function of the applied dc magnetic field ($H_{max} = 35$ Oe) at different frequencies up to $f = 10$ MHz for all the samples investigated. Figure 4 shows the frequency dependence of the maximum value of MI ratio (i.e., $[\Delta Z/Z(\%)]_{max}$) for the samples. It can be seen that $[\Delta Z/Z(\%)]_{max}$ starts to increase with increasing frequency up to 5 MHz and then decreases at higher frequencies.

This feature can be explained by considering the model of skin effects for thin ribbons.¹² Within the framework of this model, at sufficiently high frequencies (the order of MHz), the cross section through which an ac current $I = I_0 \exp(-j\omega t)$ flows is reduced due to the generation of eddy current and, consequently, the current flows through a thin sheath near the surface of the ribbon because of the skin effect. By solving the classical Maxwell equations of electrodynamics, the ac impedance $Z = R + j\omega L$ (R and L are resistance and inductance, respectively) of the ribbon can be expressed in the form

$$Z = R_{dc} \cdot jka \coth(jka), \quad (2)$$

where $2a$ is the thickness of the ribbon, R_{dc} is the electrical resistance for a dc current, $k = (1+j)/\delta_m$ with imaginary unit j , δ_m is the penetration depth in a magnetic medium with the transverse permeability of μ_T and conductivity of σ and is expressed as

$$\delta_m = \frac{c}{\sqrt{2\pi\omega\sigma\mu_T}}, \quad (3)$$

where c is the speed of light and $f = 2\pi\omega$ is the frequency of the ac current.

At a given frequency, the application of a dc magnetic field (H_{dc}) changes the transverse permeability μ_T and hence the magnetic penetration depth δ_m that in turn alters the magnetoimpedance until the value of δ_m reaches the half thickness of the sample (a). At high frequency ($\delta_m \ll a$), Eq. (3) is reduced to the expression of $Z \propto (f\mu_T)^{1/2}$. This means that, in this frequency region, the total impedance is proportional to the square root of the transverse permeability.^{12,13} Based on these analyses, it is pointed out that the GMI effect can be achieved when μ_T is large and δ_m and R_{dc} are small.

In this context, the GMI results can be interpreted by considering the change in δ_m in relation to the change of μ_T caused by the application of an external magnetic field according to Eq. (3). At frequencies below 1 MHz ($a < \delta_m$), the maximum value of GMI, $[\Delta Z/Z(\%)]_{max}$, was relatively low due to the contribution of the induced magnetoinductive voltage to magnetoimpedance. When $1 \text{ MHz} \leq f \leq 5 \text{ MHz}$ ($a \approx \delta_m$), the skin effect is dominant, a higher $[\Delta Z/Z(\%)]_{max}$ was found. Beyond $f = 5 \text{ MHz}$, $[\Delta Z/Z(\%)]_{max}$ decreases with increasing frequency (see Fig. 4). It is believed that, in this frequency region ($f \geq 5 \text{ MHz}$), the domain wall displacements were strongly damped owing to eddy currents, thus contributing less to the transverse permeability (μ_T), i.e., a small $[\Delta Z/Z(\%)]_{max}$. Furthermore, the highest value of $[\Delta Z/Z(\%)]_{max}$ corresponds to the largest value of μ_T according to Eq. (3). Meanwhile, the transverse permeability (μ_T) is directly proportional to the longitudinal permeability due to rotational magnetization (μ_{hi}).¹⁴ Therefore, the largest value of $[\Delta Z/Z(\%)]_{max}$ corresponds to the largest value of μ_{hi} . As one can see from Table I, the nanocrystalline sample (No. 4) among the samples investigated has the largest value of μ_{hi} thus resulting in the largest value of $[\Delta Z/Z(\%)]_{max}$. As compared with the as-quenched sample (No. 1), $[\Delta Z/Z(\%)]_{max}$ is considerably larger in the neutron-irradiated sample (No. 3) and is likely due to the higher value of μ_{hi} (see Table I). The decrease of μ_{hi} and the increase of H_c in the 823 K-annealed alloy after neutron irradiation (No. 5) lead to a considerable reduction in $[\Delta Z/Z(\%)]_{max}$, as compared to the 823 K-annealed alloy (No. 4).

In the present work, it should be emphasized that amorphous alloys increase their permeability upon neutron irradiation, while nanocrystalline alloys decrease their permeability upon neutron irradiation. This fact has important consequences in the application of these materials as sensing

elements in a nuclear environment when the magnetoimpedance effect is used,^{13,15} because, when compared with the annealed amorphous alloy, the amorphous materials are less brittle and easier to handle which provides the necessary manufacturing flexibility and, more importantly, their magnetoimpedance properties can be enhanced by subsequent neutron irradiation.

The authors are grateful to Dr. B. G. Kim (HANARO center, Korea Atomic Energy Research Institute, Taejon 305-600, South Korea) for the neutron irradiation experiments. This work was partially supported by the Korea Science and Engineering Foundation through the Research Center for Advanced Magnetic Materials at Chungnam National University.

*Corresponding author. Electronic address:
M.H.Phan@bristol.ac.uk

¹M. E. McHenry, M. A. Willard, and D. E. Laughlin, *Prog. Mater. Sci.* **44**, 291 (1999).

²T. A. Donnelly, D. G. Fisher, R. B. Murray, and C. P. Swann, *J. Appl. Phys.* **53**, 7801 (1982).

³D. G. Fisher, R. B. Murray, and C. P. Swann, *J. Appl. Phys.* **56**, 1055 (1984).

⁴R. D. Brown, J. R. Cost, and J. T. Stanley, *J. Appl. Phys.* **55**, 1754 (1984).

⁵D. G. Fisher, R. B. Murray, and C. P. Swann, *J. Appl. Phys.* **58**, 460 (1985).

⁶C. G. Kim, H. C. Kim, S. S. Yoon, D. G. Park, and J. H. Hong, *J. Magn. Magn. Mater.* **203**, 217 (1999).

⁷Y. S. Kim, M. H. Phan, S. C. Yu, K. S. Kim, H. B. Lee, B. G. Kim, and Y. H. Kang, *Physica B* **327**, 311 (2003).

⁸Y. Yoshizawa, S. Oguma, and K. Yamauchi, *J. Appl. Phys.* **64**, 6044 (1988).

⁹C. G. Kim, S. S. Yoon, and S. C. Yu, *Appl. Phys. Lett.* **76**, 3463 (2000).

¹⁰K. S. Byon, S. C. Yu, J. S. Kim, and C. G. Kim, *IEEE Trans. Magn.* **36**, 3439 (2000).

¹¹M. H. Phan, S. C. Yu, C. G. Kim, and M. Vázquez, *Appl. Phys. Lett.* **83**, 2871 (2003).

¹²L. V. Panina, K. Mohri, T. Uchiyama, and M. Noda, *IEEE Trans. Magn.* **31**, 1249 (1995).

¹³M. Knobel and K. R. Pirota, *J. Magn. Magn. Mater.* **242-245**, 33 (2002).

¹⁴M. H. Phan, H. X. Peng, M. R. Wisnom, S. C. Yu, and N. H. Nghi, *Sens. Actuators* (to be published).

¹⁵P. Marin and A. Hernando, *J. Magn. Magn. Mater.* **215-216**, 729 (2000).